

Remaining Useful Life Prediction for Proton Exchange Membrane Fuel Cells Including Reversible and Irreversible Losses

Abdelkader Detti^{1,2}, Elodie Pahon^{1,2}, Nadia Yousfi Steiner^{1,2}, Samir Jemei^{1,2}, Laurent Bouillaut^{3,*}, Allou Badara Same³, Daniel Hissel^{1,2}

¹Franche-Comte Electronics Mechanics Thermal Science and Optics Sciences and Technologies, University of Bourgogne Franche-Comte, Belfort, France

²Fuel Cell Laboratory, University of Bourgogne Franche-Comte, Belfort, France

³Engineering of Surface Transportation Networks and Advanced Computing Laboratory, University Gustave Eiffel, Marne-la-Vallée, France

Email address:

haidar.detti@gmail.com (A. Detti), elodie.pahon@femto-st.fr (E. Pahon), nadia.steiner@femto-st.fr (N. Y. Steiner), samir.jemei@femto-st.fr (S. Jemei), laurent.bouillaut@univ-eiffel.fr (L. Bouillaut), allou.same@univ-eiffel.fr (A. B. Same), daniel.hissel@femto-st.fr (D. Hissel)

*Corresponding author

To cite this article:

Abdelkader Detti, Elodie Pahon, Nadia Yousfi Steiner, Samir Jemei, Laurent Bouillaut, Allou Badara Same, Daniel Hissel. Remaining Useful Life Prediction for Proton Exchange Membrane Fuel Cells Including Reversible and Irreversible Losses. *International Journal of Energy and Power Engineering*. Vol. 11, No. 2, 2022, pp. 39-46. doi: 10.11648/j.ijjepe.20221102.13

Received: February 21, 2022; **Accepted:** March 9, 2022; **Published:** April 20, 2022

Abstract: Today the world is full of time-dependent phenomena in all fields: physics, chemistry, mechanics and many others. Time acts on the performance of any system whatever its nature is. Moreover, proton exchange membrane fuel cells are promising alternatives to conventional power sources due to their high energy density and zero gas emission. However, this technology is still not sufficiently mature to reach large-scale deployment due to its limited lifespan. To extend the lifespan, the “Prognosis and Health Management” discipline has been developed, which is considered to be efficient in improving the reliability, durability and maintainability of fuel cell systems. However, it involves a deep understanding of the reversible and irreversible degradation phenomena and their impacts on fuel cell performance. Based on this, this paper deals with analyses of reversible and irreversible degradation. The criticalities of these losses and their impacts on the fuel cell lifetime are underlined with a useful lifetime estimation based on an autoregressive moving average model. Indeed, to do so, three scenarios are studied. First, the remaining useful life is predicted by taking into account only reversible degradation, and this gives the minimum lifetime. Second, the real remaining useful life is estimated by taking into account both reversible and irreversible degradation. Finally, the maximum lifetime that can be reached is estimated by taking into account only irreversible degradation.

Keywords: Prognostics, Proton Exchange Membrane Fuel Cell, Reversible/Irreversible Degradation, Remaining Useful Life, Fuel Cell Ageing

1. Introduction

One of the major problems facing humanity is global warming, which is caused by intensive use of fossil fuels emitting huge amounts of greenhouse gases. To face this problem, new technologies and new alternatives are making their way into the energy market. However, fuel cells provide a more promising alternative that is increasingly being

considered and investigated in research and industry. Despite its various advantages, it is still limited in terms of large deployment. Cost, durability and reliability are the main barriers to scale-up of fuel cell technologies [1]. In the last decade, significant progress has been made in achieving the required costs and durability in automotive and stationary applications of proton exchange membrane fuel cells (PEMFCs) [2]. For PEMFC technology, the cost can be split into three parts: these are stack parts, electrochemical

packages comprising membrane electrode assemblies (MEAs) and gas diffusion layers (GDLs) and machine setups. The cost of the stack parts represents 47% of the final cost, the electrochemical package accounts for 33%, and the machine setup accounts for 20%. [3]. Thus, research deals with catalyst loadings [4-6] and use of platinum-free catalysts [7-9]. With respect to the membrane cost, the resistance of the membrane is reduced when its thickness is reduced. This process allows an increase in the performance of the fuel cell but affects its overall cost [10]. Moreover, the membrane electrode assembly (MEA) still exhibits limited durability due to the various degradation phenomena that occur during its operation [11, 12]. The membrane quality and state greatly influence fuel cell performance. Performance can be characterized by MEA parameters, including ohmic resistance, hydrogen crossover current, double layer capacitance, and catalyst roughness factor [13]. Membranes can be susceptible to three types of degradation: chemical, mechanical and thermal degradation. The production of hydrogen peroxide during fuel cell operation is one of the root causes of chemical membrane degradation. Futter et al. [12] proposed a physics-based model of chemical membrane degradation by taking into account the influence of pressure, relative humidity and cell voltage. Frensch et al. [14] investigated the influence of hydrogen peroxide and iron ions on fluoride emission in ex situ and in situ experiments and with a computational model. Li et al. [15] proposed a three-dimensional model with a thin MEA. A thin membrane results in low ohmic resistance and is more easily hydrated under low humidity but can suffer from hydrogen crossover. Lim et al. [16] studied membrane degradation during combined chemical and mechanical accelerated stress testing of PEMFCs. The experimental test consists of performing open-circuit voltage cycling combined with high temperature/low relative humidity conditions. Venkatesan et al. [17] studied the effects of isolated chemical and mechanical degradation stressors on the ionomer morphology in fuel cell membranes. Several remarks were offered: i) hydrophilic pores are dilated by chemical degradation, ii) mechanical degradation increases water uptake without major changes in morphology, and iii) chemically degraded ionomers are susceptible to damage by mechanical stress. Singh et al. [18] tracked the evolution of mechanical degradation in fuel cell membranes using 4D in situ visualization. Accelerated stress tests were performed to periodically track membrane mechanical degradation. The location of membrane cracking was shown to be strongly correlated with beginning-of-life MEA defects. Unlike crack initiation, crack propagation in the membranes does not appear to be significantly influenced by electrode morphology. Khorasany et al. [19] exposed MEAs to cyclic uniaxial tension at controlled temperature and relative humidity to study the effects of cyclic stresses on the fatigue and mechanical stability of perfluorosulfonic acid membranes. The fatigue lifetime was measured in terms of the number of cycles before ultimate fracture. The fatigue lifetime increased exponentially while reducing stresses. The

effect of temperature was mentioned as a more significant stress than humidity, and it caused a reduced fatigue lifetime at high temperatures. Khetabi et al. [20] reviewed the effects of mechanical compression on the performance of polymer electrolyte fuel cells and analysed them with in situ characterization techniques. They detailed the sources of mechanical stress, their respective impacts and the effects of mechanical compression on GDL characteristics.

To address the durability problem, the discipline of Prognosis and Health Management (PHM) has been developed. It aims at predicting fuel cell performance and constructing new degradation indicators [21]. Sutharssan et al. [22] proposed a review on PHMs dedicated to PEMFCs. Different approaches can be used for prognostics of PEMFC in order to forecast the remaining useful life (RUL) of the system. The RUL is the time before failure of the system or the time when the fuel cell system loses 10% of its initial power [23]. To perform lifetime prediction, data-based or non-data-based approaches can be used. Robin et al. [24] developed a multiscale model of catalyst dissolution that is coupled to a dynamic fuel cell model to predict the performance loss of PEMFCs. They simulated the equivalent active surface area loss and compared it with durability tests. Javed et al. [25] proposed a data-driven approach for prognostics of PEMFC stacks using an ensemble of constraint-based Summation Wavelet-Extreme Learning Machine (SW-ELM) models. Regarding model-based approaches, Mao et al. [26] investigated variations in PEMFC internal behaviour under different operating conditions to predict future fuel cell performance. Liu et al. [27] presented an efficient semi-empirical model-based prognostics method estimating the health state and the remaining useful life of PEMFCs based on the adaptive unscented Kalman filter algorithm.

To obtain an accurate estimation of the remaining useful life of a fuel cell, a good understanding of the degradation phenomenon is required so as to take good corrective actions and extend the lifetime. However, this is a tricky task because of the numerous and different phenomena involved. They can be chemical, mechanical or thermal in nature [28]. Furthermore, the reversibility of degradation must be taken into account [29]. Indeed, during operation, a fuel cell is subject to several degradation phenomena that can be eliminated; these are known as reversible degradations, such as flooding or drying [30]. Other degradations cannot be eliminated. For example, irreversible degradations are related to the ageing of the fuel cell and are connected to physical degradations of the fuel cell, such as loss of active area, carbon corrosion or even catalyst layer poisoning [31]. Dijoux et al. [32] proposed a table in which reversibility and the parameters involved in each kind of fault appearing in a fuel cell system were detailed.

The purpose of this paper is to highlight the difference between the reversible and irreversible degradation of fuel cells. To do so, a long-term experiment is performed with periodic characterization used to manage fuel degradation. Some reversible losses are observed after each characterization. A

complete study of reversible and irreversible losses is performed to better understand recovery phenomena. On the other hand, an estimation of the remaining useful life is performed by taking into account reversible degradation and then the irreversible degradation that gives the maximum lifetime of the tested fuel cell.

This paper is organized as follows; the experimental details are presented in the first section. The second section deals with the analysis of reversibility and irreversibility of fuel cell degradations. Then, the prognostic approach and the results are presented.

2. Description of the Experimental Equipment

The fuel cell was run at the nominal operating conditions, i.e., with a constant current density of 0.6 A/cm^2 , a temperature of 60°C , and a relative humidity at the cathode side of 70%; at the anode side, the hydrogen was dried, and pressures were 1.5 bars on both sides and stoichiometries of 1.5 and 2 were used for the anode and cathode, respectively.

Table 1. Summarises the 5-cell stack specifications.

Parameter	Value
Number of cell	5
Active area	100 cm^2
Anode stoichiometry	1.5
Cathode stoichiometry	2
Inlet air pressure (abs.)	1.5 bars
Inlet hydrogen pressure (abs.)	1.5 bars
Maximal difference pressure between both compartments	50 kPa
Stack temperature	60°C
Anode relative humidity	0%
Cathode relative humidity	70%
Current density	0.6 A/cm^2

Over time, the fuel cell naturally aged, and its performance decreased. The total time of the experiment was 1800 hours (figure 1). The voltage drop for the stack was 0.54 V , a degradation of $60 \mu\text{V/cell/h}$. The power loss was approximately 36 W , which corresponded to 18%.

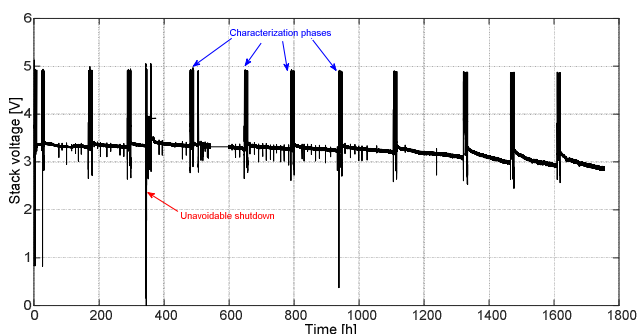


Figure 1. 5-cell stack ageing experiment.

Nevertheless, strong misunderstandings of this multiphysical and multiscale system imply that no one can predict the rate of degradation of this fuel cell. Degradation markers were collected weekly on the system. They enhanced

the base of information needed for the prognostics.

Several measurements were made each week on a polarization curve ranging between 0 and 0.9 A/cm^2 and electrochemical impedance spectra (EIS) at five current densities: 0.2 , 0.4 , 0.6 , 0.8 and 0.9 A/cm^2 . These characterisations were made successively on a single day. EIS was performed with an in-lab spectrometer that performed EIS with each cell and for the whole stack. EIS was performed at 0.9 A/cm^2 at the beginning of life, since the maximal current density was 1.1 A/cm^2 .

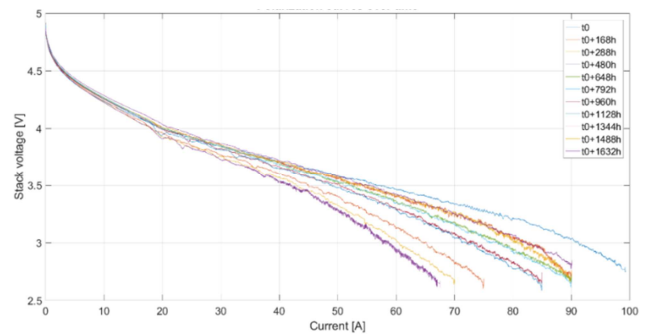


Figure 2. Polarisation curves over time for the 5-cell stack.

Obviously, this current density value could not be realized during the complete ageing test, since the fuel cell degraded over time.

Figure 2 presents the evolution of the stack voltage as a function of current for various times. The maximal current that the fuel cell achieved decreased over time. This limit was fixed by a minimum voltage threshold fixed at 0.4 V/cell .

3. Reversible and Irreversible Performance Losses

3.1. Definition of Reversible and Irreversible Losses

It is important to emphasize that after each characterization phase, the stack voltage was higher than the stack voltage just before the characterization phase. Thus, the characterizations acted as a recovery protocol for the fuel cell. Jouin *et al.* [33] mentioned this and made it clear that the power recovery of the fuel cell stack also depends on ageing. This means that the fuel cell stack does not recover the same performance ratio after each characterization. Reversible losses are caused by the change in operating conditions during characterizations. Indeed, during the static characterization of the fuel cell (polarization curve), the whole range of the current density was considered. This leads to better humidification of the membrane and thus improves the fuel cell performance during a specific time. Figure 3 shows these phenomena in the long-term experiment running under a constant load.

In the literature, several other durability tests on fuel cell stacks led to the same observations [34]. Liu *et al.* [35] tested a 25 cm^2 single-cell PEMFC with the “MEA/Stack Durability Protocol” developed by the Fuel Cell Technical Team [2], which comprised wet and dry load cycling. At the beginning

of life, the performance was 0.8 V@100 mA/cm², whereas the performance decreased to 0.7 V@100 mA/cm² after 210 hours of run time (end of the test).

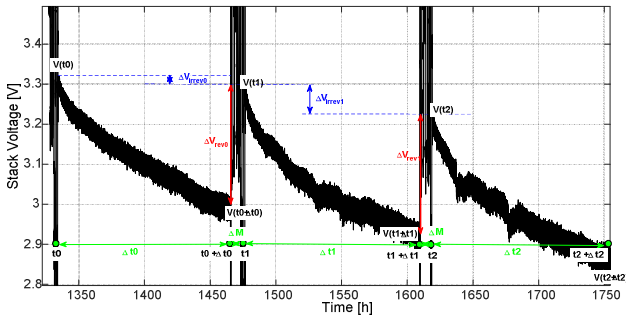


Figure 3. Reversible and irreversible voltage losses of the 5-cell stack under a constant load.

The overall voltage decay rate was approximately 0.48 mV/h. The voltage drop phenomenon resulted from both irreversible durability decay and also reversible stability decay, with some recoveries occurring after the interruption for diagnostic testing or low voltage. Cleghorn et al. [36] presented the results of a 26,300-hour 25 cm² PEM single-cell lifetime test operated with a commercial MEA under conditions relevant to stationary fuel cell applications. The degradation rate for total performance was between 4 and 6 μ V/h @ 800 mA/cm². Again, different voltage decays were observed over time, which were more or less important. Hu et al. [37] presented interesting experimental results obtained with a two-cell PEMFC with an area of 335 cm². They analysed the voltage degradation rates for several 100-hours periods of time. Depending on the interval number, the absolute value of the degradation rate for cell 1 was 25 μ V/h, and it was 35 μ V/h for cell 2 in the complete test. Dubau et al. [38] performed a long-term test (12,860 h) on a 110-cell PEMFC stack (86 cm²) under a constant load ($j=0.25$ A/cm²). The overall degradation rate was approximately 3.5 μ V/h, but there was such large heterogeneity of performance, especially in the first and last 3,000 hours. Liu et al. [39] and Lechartier et al. [40] presented results on a 1 kW-PEMFC stack (100 cm²). The degradation observed for the stack voltage over 1154 hours was again nonlinear.

This suggests that the voltage degradation was composed of reversible and irreversible losses. A clear definition of reversible and irreversible losses and calculations were proposed in the Science for Policy report by the Joint Research Center, the in-house science service of the European Commission [41].

The reversible voltage losses result from transient processes. Their impact on the stack voltage is observable. However, this voltage loss can be reversed by changing the operating conditions or by using a recovery procedure. One of the most common reversible degradations concerns the water management of the system. Membrane humidification varies during static characterization, and it could explain the performance recovery [33]. ΔV_{rev} is the recoverable part of the voltage. It is the difference between the starting voltage

$V(t_i+1)$ and the ending previous voltage $V(t_i+\Delta t_i)$.

Irreversible voltage losses are often associated with natural ageing. Indeed, irreversible degradation includes irreversible changes in the fuel cell components and materials, such as pinhole formation in the membrane, platinum migration or carbon corrosion [42]. ΔV_{irrev} is the non-recoverable part of the voltage. It is the difference between the starting voltage $V(t_i)$ and the ending voltage $V(t_i+1)$. Both reversible and irreversible degradation lead to voltage decay; therefore, it is important to determine the difference when voltage decay is observed and whether it is due to reversible or irreversible degradation. Equations 1 to 4 give show the calculations of reversible and irreversible voltage losses, the total irreversible voltage loss and the degradation rate.

$$\Delta V_{rev,i} = V(t_{i+1}) - V(t_i + \Delta t_i) \text{ in } \mu\text{V} \quad (1)$$

$$\Delta V_{irrev,i} = V(t_i) - V(t_{i+1}) \text{ in } \mu\text{V} \quad (2)$$

$$\Delta V_{irrev,tot} = \sum_{i=1}^N \Delta V_{irrev,i} \text{ in } \mu\text{V} \quad (3)$$

$$V_{irrev,tot} = \frac{\sum_{i=1}^N \Delta V_{irrev,i}}{\sum_{i=1}^N \Delta t_i} \text{ in } \mu\text{V/h} \quad (4)$$

3.2. Analysis of Reversible and Irreversible Losses

Based on the definition given in the previous section, the reversible and irreversible losses were calculated in the long-term experiment. In figure 4, several intervals are defined. They correspond to periods during which the fuel cell ran under the nominal operating conditions and under constant load. For each continuous part, the degradation rate (denoted λ in table 2), voltage losses and reversible and irreversible losses were calculated by using equations 1, 2 and 4 and expressed in mV/h and V, respectively. Table 2 presents the results. For reversible losses, the sign “+” is conventionally added as the performances are recovered, whereas for irreversible losses, the sign “-” is conventionally added as the performance remains lower.

At interval No. 0 (conditioning phase of the fuel cell), the reversible losses are null because a first characterization (recovery phase) is needed to observe the recoverable voltage. Thus, during the first 24 hours, only the voltage was ageing in the fuel cell, which is considered an irreversible loss. It is not possible to calculate the irreversible losses for the last interval of time (No. 13) because the voltage value after the last characterization phase is unknown.

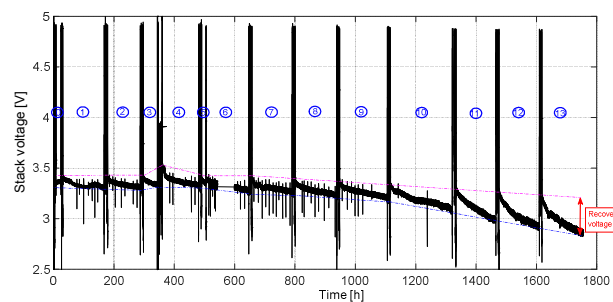


Figure 4. Stack voltage evolution with a recoverable voltage threshold and continuous operation parts.

Depending on time, the reversible and irreversible losses are different even for the same interval of time. Generally, the reversible losses increased over time from 0.041 V at the BOL to approximately 0.3 V at the end of the test, while the irreversible losses were quite similar over time. For interval No. 4, both reversible and irreversible losses were high due to an unavoidable shutdown that occurred during

the experimental test. After the 10% power loss (interval Nos. 11, 12 & 13), both reversible and irreversible losses increased significantly. Thus, the fuel cell performance recovery was higher but occurred during a shorter time (one day), which finally resulted in higher irreversible losses. The trend for the last three parts was more severe than the previous ones.

Table 2. Degradation rate (λ) and different loss expressions.

N#	Interval (h)	λ (mV/h)	Voltage losses (V)	Reversible losses (V)	Irreversible losses (V)
0	8→24	+1.7	+ 0.027	0	+ 0.068
1	31→167	-0.7	- 0.099	+ 0.041	- 0.005
2	180→287	-0.8	- 0.088	+ 0.094	+ 0.001
3	298→344	-1.4	- 0.065	+ 0.089	+ 0.294
4	361→480	-3.1	- 0.37	+ 0.359	- 0.308
5	491→504	-3.5	- 0.045	+ 0.062	+ 0.005
6	506→647	-0.9	- 0.124	+ 0.05	- 0.004
7	658→790	-0.9	- 0.12	+ 0.12	- 0.023
8	800→938	-1	- 0.138	+ 0.97	- 0.013
9	948→1106	-0.9	- 0.142	+ 0.125	- 0.02
10	1116→1321	-1.2	- 0.248	+ 0.122	- 0.033
11	1334→1466	-2.4	- 0.313	+ 0.215	- 0.031
12	1477→1610	-2.6	- 0.347	+ 0.282	- 0.069
13	1619→1755	- 2.5	- 0.341	+ 0.278	X
Total	8→1755	- 0.3	- 0.479	1.934	- 0.138

4. Prognostic Approach

The discipline of Prognosis and Health Management (PHM) aims to extend the reliability and lifetime of engineering systems by monitoring and predicting their degradation. It also allows the construction of new degradation indicators. For fuel cells, PHM is used to estimate their RUL, schedule maintenance and improve their durability. This work focuses on prognosis, which can be categorized into three main approaches: (i) model-based, (ii) data-based and (iii) hybrid. The use of a model-based approach requires deep physical knowledge of the system studied, and it is also called the white box model [28]. The combination of data and a prediction process is a data-based approach that will be used in this study and does not require any physical knowledge of the studied system. This approach is also called a black-box model [44]. Finally, the combination of the two previous approaches results in the hybrid approach [44].

In this work, an autoregressive moving average (ARMA) model was used to predict the voltage degradation and estimate the RUL of a fuel cell stack. Indeed, the ARMA model has proven its prediction accuracy in various fields [45-47]. It describes a stochastic stationary process varying with time.

The autoregressive AR(p) process describes an observation X_t as a linear function of previous observations X_{t-k} and white noise, according to the following equation:

$$X_t = \sum_{k=1}^p \varphi_k X_{t-k} + \varepsilon_t \quad (5)$$

The Moving Average part has been first introduced by Slutsky [48] according to the following equation:

$$X_t = \sum_{k=1}^q \theta_k X_{t-k} + \varepsilon_t \quad (6)$$

Where φ_k and θ_k ($k=1,2,\dots,q$) are respectively the autoregressive and moving-average processes parameters, X_{t-k} is the observation “ k ” time-units before the current time “ t ” and ε_t is a white noise which has independent and identical distribution with X_t , $\mathbb{E}(\varepsilon_t) = 0$, $\text{Var}(\varepsilon_t) = \sigma^2 > 0$.

The ARMA model, a combination of the two last processes, used the first time by Yule [49] to model the number of sunspot time series. It describes future variable values with a linear function which depends on previous observation and random errors according to the following equation:

$$X_t = \sum_{k=1}^p \varphi_k X_{t-k} + \sum_{k=1}^q \theta_k X_{t-k} + \varepsilon_t \quad (7)$$

This study is aimed at prediction of the voltage degradation and accurate estimation of the RUL of the tested fuel cell stack. This estimation remains difficult due to the various phenomena that occur during fuel cell operation. Some of these phenomena are reversible, and others are not. In the rest of the paper, the conditioning phase will be removed from our study. The interval time No. 1 will be considered the beginning of the life of the fuel cell stack.

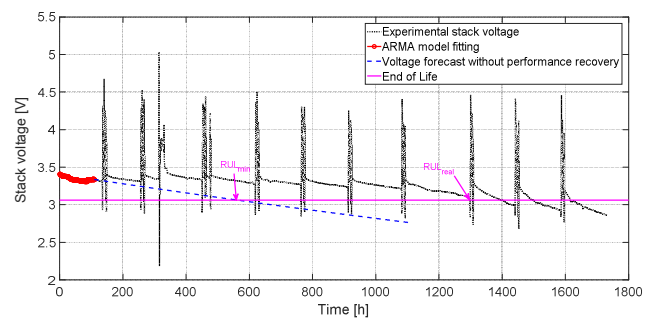


Figure 5. RUL estimation without performance recovery.

In the first time period, the RUL estimation was done without taking into account the performance recovery; in other words, the prediction was done by considering the reversible degradation. To ensure that the ARMA model was adjusted only on the first part of the voltage signal (interval No. 1) lasting for 136 hours, the prediction phase began just before the characterization between intervals No. 1 and No. 2. The RUL estimation, represented in Figure 5, was computed with reference to the end of life (EOL), which corresponds to a 10% loss in stack power. In this case, this corresponds to a voltage of 3.065 V. The RUL estimation gave a value of 560 operating hours, which is denoted as RUL_{min} .

To obtain a precise estimation of RUL that was closer to reality (1320 h), performance recovery had to be considered in the adjustment of the ARMA model. In this case, the prediction phase began after the fifth characterization (after interval No. 6), as represented in Figure 6. The learning phase of the ARMA model was approximately 40% of the total signal length (720 hours), and the prediction was performed 100 steps ahead. The results obtained corresponded to the RUL_{real} , with a mean square error MSE of 0.0002% compared with the experimental data.

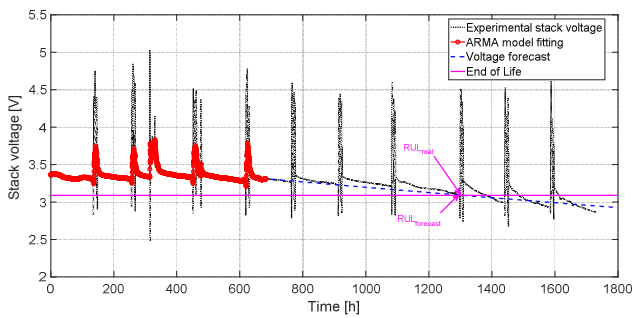


Figure 6. RUL estimation with consideration of reversible and irreversible losses.

The last step is to estimate the RUL of the tested stack by considering only irreversible degradation. The voltage signal was computed by picking up the upper voltage value reached after each characterization (12 values or samples). The ARMA model was adjusted to the 11th sample, which corresponded to the irreversible voltage obtained at the beginning of interval No. 12 and further predicted the 12th sample. The prediction gave the exact voltage value resulting after the last characterization (No. 13). A further prediction computed for 2240 operating hours allowed us to estimate the third RUL denoted RUL_{max} , which corresponded to 2100 operating hours, as illustrated in Figure 7.

The maximum RUL is supposed to be real if fuel cell operation is not subjected to degradation phenomena. It can be associated with the maximal RUL value that can be achieved. However, this value does not correspond to reality due to other phenomena that occur during operation; it is associated with the natural ageing of the fuel cell stack. Reversible degradation phenomena are unavoidable but can be minimized by applying characterization or shutdown phases.

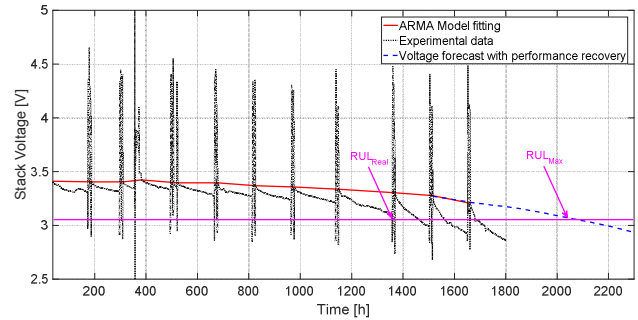


Figure 7. EIS during the second test campaign.

When no characterization or shutdown is applied to the fuel cell stack during its operation, there will be an accumulation of reversible degradations, which leads to a significant performance loss. This accumulation results in irreversible degradation and thus leads to reduced stack RUL, which explains the characterization RUL_{min} .

5. Conclusions

The study of reversible and irreversible degradations as well as the prediction of performance and the estimation of remaining useful life are the subjects of various research works. In this study, these different issues were highlighted. First, the results of experimental ageing tests were presented; based on those data, reversible and irreversible aspects of the degradation were explained and analyzed.

This analysis allowed computation of the degradation rate of the tested stack over time, which saw exponential growth after having reached a loss of 10% of the BOL power of the stack. The effect of reversible and irreversible degradation was highlighted by estimating the RUL, according to three scenarios that resulted in the three RUL values.

The first case corresponded to operation without recovery performance, which resulted in a consistent loss of fuel cell performance. In this case, the RUL was approximately 600 hours, but this remains a theoretical result. This scenario is unlikely to exist in a fuel cell application, either for stationary applications or an automotive application. In this study, the parameter RUL_{min} was computed only for comparison purposes. To extend the fuel cell lifetime, some characterizations or shutdowns might be performed, which would lead to recovery of the fuel cell performance.

The second case considered both reversible and irreversible losses and represents the real degradation of a fuel cell stack. Over time and after the characterization steps, some voltage recovery was observed. In this case, the RUL was 1320 hours, based on the end-of-life definition. The last case considered performance losses caused by stack ageing. In this case, the RUL was maximal and was equal to 2100 hours, which corresponded to a gain of 60% versus the real RUL if perfect recovery performance is expected. Consequently, it is necessary to consider reversibility phenomena to estimate the real lifetime of a fuel cell, as the RUL can vary by $\pm 50\%$ from the real one. According to the results obtained, the significant gap between RUL_{max} and RUL_{real} needs further investigation. Thus, the

recovery performance protocol is an issue requiring development in order to extend the durability of the fuel cell stack.

Acknowledgements

The authors gratefully acknowledge the Bourgogne Franche-Comté region and the EIPHI Graduate School (contract "ANR-17-EURE-0002"), which enabled the realization of this work and the corresponding experimental campaigns.

References

- [1] Wu J., Yuan X. Z., Martin J. J., Wang H., Zhang J., Shen J., Wu S., Merida W. (2008). *A review of PEM fuel cell durability: Degradation mechanisms and mitigation strategies*, Journal of Power Sources, Vol. 184 (1), pp. 104-119.
- [2] "DOE Hydrogen 2017". Fuel cell Technical Team Roadmap, 2017, pp. 1-38.
- [3] Giacoppo G., Hovland S., Barbera O. (2019). *2 kW modular PEM fuel cell stack for space applications: Development and test for operation under relevant conditions*, Applied Energy, Vol. 242, pp. 1683-1696.
- [4] Gasteiger H. A., Panels J. E., Yan S. G. (2004). *Dependence of PEM fuel cell performance on catalyst loading*, Journal of Power Sources, Vol. 127 (1-2), pp. 162-171.
- [5] Zhang Y., Smirnova A., Verma A., Pitchumani R. (2015). *Design of a proton exchange membrane (PEM) fuel cell with variable catalyst loading*, Journal of Power Sources, Vol. 291, pp. 46-57.
- [6] Stocker M. T., Barnes B. M., Sohn M., Stanfield E., Silver R. M. (2017). *Development of large aperture projection scatterometry for catalyst load evaluation in proton exchange membrane fuel cells*, Journal of Power Sources, Vol. 364, pp. 130-137.
- [7] Zhang S., Yuan X. Z., Hin J. N. C., Wang H., Friedrich K. A., Schulze M. (2009). *A review of platinum-based catalyst layer degradation in proton exchange membrane fuel cells*, Journal of Power sources, Vol. 194 (2), pp. 588-600.
- [8] Majlan E. H., Rohendi D., Daud W. R. W., Husaini T., Haque M. A. (2018). *Electrode for proton exchange membrane fuel cells: A review*, Renewable and Sustainable Energy Reviews, Vol. 89, pp. 117-134.
- [9] Stariha S., Artyushkova K., Workman M. J., Serov A., Mckinney S., Halevi B., Atanassov P. (2016). *PGM-free Fe-N-C catalysts for oxygen reduction reaction: Catalyst layer design*, Journal of Power Sources, Vol. 326, pp. 43-49.
- [10] Ogungbemi E., Ijaodola O., Khatib F. N., Wilberforce T., El Hassan Z., Thompson J., Ramadan M., Olabi A. G. (2019). *Fuel cell membranes - Pros and cons*, Energy, Vol. 172, pp. 155-172.
- [11] Vilekar S. A., Datta R. (2010). *The effect of hydrogen crossover on open-circuit voltage in polymer electrolyte membrane fuel cells*, Journal of Power Sources, Vol. 195 (8), pp. 2241-2247.
- [12] Futter G. A., Latz A., Jahnke T. (2016). *Physical modeling of chemical membrane degradation in polymer electrolyte membrane fuel cells: Influence of pressure, relative humidity and cell voltage*, Journal of Power Sources, Vol. 410-411, pp. 78-90.
- [13] Wu Z., Pei P., Xu H., Jia X., Ren P., Wang B. (2019). *Study on the effect of membrane electrode assembly parameters on polymer electrolyte membrane fuel cell performance by galvanostatic charging method*, Applied Energy, Vol. 251, pp. 313-320.
- [14] Frensch S. H., Serre G., Fouda-Onana F., Jensen H. C., Christensen M. L., Araya S. S., Kaer S. K. (2019). *Impact of iron and hydrogen peroxide on membrane degradation for polymer electrolyte membrane water electrolysis: Computational and experimental investigation on fluoride emission*, Journal of Power Sources, Vol. 420, pp. 54-62.
- [15] Li Y., Zhou Z., Liu X., Wu W. T. (2019). *Modeling of PEM fuel cell with thin MEA under low humidity operating condition*, Applied Energy, Vol. 242, pp. 1513-1527.
- [16] Lim C., Ghassemzadeh L., Van F. Hove, Lauritzen M., Kolodziej J., Wang G. G., Holdcroft S., Kjeang E. (2014). *Membrane degradation during combined chemical and mechanical accelerated stress testing of polymer electrolyte fuel cells*, Journal of Power Sources, Vol. 257, pp. 102-110.
- [17] Venkatesan S. V., Kjeang E. (2017). *Effects of isolated chemical and mechanical degradation stressors on the ionomer morphology in fuel cell membranes*, Polymer Degradation and Stability, Vol. 146, pp. 132-139.
- [18] Singh Y., White R. T., Najm M., Haddow T., Pan V., Orfino F. P., Dutta M., Kjeang E. (2019). *Tracking the evolution of mechanical degradation in fuel cell membranes using 4D in situ visualization*, Journal of Power Sources, Vol. 412, pp. 224-237.
- [19] Khorasany R. M. H., Alavijeh A. S., Kjeang E., Wang G. G., Rajapakse R. K. N. D. (2015). *Mechanical degradation of fuel cell membranes under fatigue fracture tests*, Journal of Power Sources, Vol. 274, pp. 1208-1216.
- [20] Khetabi E. M., Bouziane K., Zamel N., François X., Meyer Y., Candusso D. (2019). *Effects of mechanical compression on the performance of polymer electrolyte fuel cells and analysis through in-situ characterization techniques - A review*, Journal of Power Sources, Vol. 424, pp. 8-26.
- [21] Mao L., Jackson L. (2016). *Selection of optimal sensors for predicting performance of polymer electrolyte membrane fuel cell*, Journal of Power Sources, Vol. 328, pp. 151-160.
- [22] Sutharssan T., Montalvao D., Chen Y. K., Wang W. C., Pisac C. (2017). *A review on prognostics and health monitoring of proton exchange membrane fuel cell*, Renewable and Sustainable Energy Reviews, Vol. 75, pp. 430-450.
- [23] Jouin M., Bressel M., Morando S., Gouriveau R., Hissel D., Péra M. C., Zerhouni N., Jemei S., Hilairet M., Ould Bouamama B. (2016). "Estimating the end-of-life of PEM fuel cells: Guidelines and metrics", Applied Energy, Vol. 177, pp. 87-97, 2016.
- [24] Robin C., Gérard M., Quinaud M., d'Arbigny J., Bultel Y. (2016). *Proton exchange membrane fuel cell model for aging predictions: Simulated equivalent active surface area loss and comparisons with durability tests*, Journal of Power Sources, Vol. 326, pp. 417-427.

- [25] Javed K., Gouriveau R., Zerhouni N., Hissel D. (2016). *Prognostics of proton exchange membrane fuel cell stack using an ensemble of constraints based connectionist networks*, Journal of Power Sources, Vol. 324, pp. 745-757.
- [26] Mao L., Jackson L., Jackson T. (2017). *Investigation of polymer electrolyte membrane fuel cell internal behavior during long term operation and its use in prognostics*, Journal of Power Sources, Vol. 362, pp. 39-49.
- [27] Liu H., Chen J., Zhu C., Su H., Hou M. (2017). *Prognostics of proton exchange membrane fuel cells using a model-based method*, IFAC-PapersOnLine, Vol. 50 (1), pp. 4757-4762.
- [28] Pei P., Chen H. (2014). *Main factors affecting the lifetime of proton exchange membrane fuel cells in vehicle applications: A review*, Applied Energy, Vol. 125, pp. 60-75.
- [29] Gazdizick P., Mitzel J., Sanchez D. G., Schulze M., Friedrich K. A. (2016). *Evaluation of reversible and irreversible degradation rates of polymer electrolyte membrane fuel cells tested in automotive conditions*, Journal of Power Sources, Vol. 327, pp. 86-95.
- [30] Sanchez D. G., Ruiu T., Biswas I., Schulze M., Helmly S., Friedrich K. A. (2017). *Local impact of humidification on degradation in polymer electrolyte fuel cells*, Journal of Power Sources, Vol. 352, pp. 42-55.
- [31] Shabani B., Hafttananian M., Khamni S., Ramiar A., Ranjbar A. A. (2019). *Poisoning of proton exchange membrane fuel cells by contaminants and impurities: Review of mechanisms, effects, and mitigation strategies*, Journal of Power Sources, Vol. 427, pp. 21-48.
- [32] Dijoux E., Yousfi-Steiner N., Benne M., Péra M. C., Grondin Pérez B. (2017). *A review of fault tolerant control strategies applied to proton exchange membrane fuel cell systems*, Journal of Power Sources, Vol. 359, pp. 119-133.
- [33] Jouin M., Gouriveau R., Hissel D., Péra M. C., Zerhouni N. (2016). *Joint particle filters prognostics for PEMFC power prediction at constant current solicitation*, IEEE Transactions on Reliability, Vol. 65 (1), pp. 336-349.
- [34] Yuan X. Z., Li H., Zhang S., Martin J., Wang H. (2011). *A review of polymer electrolyte membrane fuel cell durability test protocols*, Journal of Power Sources, Vol. 196 (22), pp. 9107-9116.
- [35] Liu M., Wang C., Xie F., Mao Z. (2013). *Polymer electrolyte fuel cell life test using accelerating degradation technique*, International Journal of Hydrogen Energy, Vol. 38 (25), pp. 11011-11016.
- [36] Cleghorn S. J. C., Mayfield D. K., Moore D. A., Rusch G., Sherman T. W., Sisofo N. T., Beuscher U. (2006). *A polymer electrolyte fuel cell life test: 3 years of continuous operation*, Journal of Power Sources, Vol. 158 (1), pp. 446-454.
- [37] Hu M., Cao G. (2014). *Research on the long-term stability of a PEMFC stack: Analysis of pinhole evolution*, International Journal of Hydrogen Energy, Vol. 39 (15), pp. 7940-7954.
- [38] Dubau L., Castanheira L., Chatenet M., Maillard F., Dillet J., Maranzana G., Abbou S., Lottin O., De Moor G., El Kaddouri A., Bas C., Flandin L., Rossinot E., Casqué N. (2014). *Carbon corrosion induced by membrane failure: The weak link of PEMFC long-term performance*, International Journal of Hydrogen Energy, Vol. 39 (36), pp. 21902-21914.
- [39] Liu J., Chen W., Yan Y., Qiu Y., Cao T. (2019). *Remaining useful life prediction of PEMFC based on long-short-term memory recurrent neural networks*, International Journal of Hydrogen Energy, Vol. 44 (11), pp. 5470-5480.
- [40] Lechartier E., Laffly E., Péra M. C., Gouriveau R., Hissel D., Zerhouni N. (2015). *Proton exchange membrane fuel cell behavioral model suitable for prognostics*, International Journal of Hydrogen Energy, Vol. 40, pp. 8384-8397.
- [41] Tsotridis G., Pilenga A., De Marco G., Malkow T. (2015). *EU harmonised test protocols for PEMFC MEA testing in single cell configuration for automotive applications*, Publications Office of the European Union.
- [42] Kundu S., Fowler M., Simon L. C., Abouatallah R. (2008). *Reversible and irreversible degradation in fuel cells during Open Circuit Voltage durability testing*, Journal of power sources, Vol. 182, pp. 254-258.
- [43] Ma R., Yang T., Breaz E., Li Z., Briois P., Gao F. (2018). *Data-driven proton exchange membrane fuel cell degradation prediction through deep learning method*, Applied Energy, Vol. 231, pp. 102-115.
- [44] Zhou D., Al-Durra A., Zhang K., Ravey A., Gao F. (2018). *Online remaining useful lifetime prediction of proton exchange membrane fuel cells using a novel robust methodology*, Journal of Power Sources, Vol. 399, pp. 314-328.
- [45] Loi T. S. A., Ng J. L. (2018). *Anticipating electricity prices for future needs - Implications for liberalized retail markets*, Applied Energy, Vol. 212, pp. 244-264.
- [46] Yang Z., Ce L., Lian L. (2017). *Electricity price forecasting by a hybrid model, combining wavelet transform, ARMA and kernel-based extreme learning machine methods*, Applied Energy, Vol. 190, pp. 291-305.
- [47] Erdem E., Shi J. (2011). *ARMA based approaches for forecasting the tuple of wind speed and direction*, Applied Energy, Vol. 88 (4), pp. 1405-1414.
- [48] Slutsky E. (1973). *The summation of random causes as the source of cyclic processes*. *Econometrica*, Vol. 5 (2), pp. 105-146.
- [49] Yule G. U. (1927). *On a method of investigating periodicities in disturbed series, with special reference to wolfer's sunspot numbers*, Philosophical Transactions of the Royal Society, Vol. 226, pp. 1-32.